Effects due to geometry and boundary conditions in multiple light scattering

C. P. Gonatas
Department of Physics–David Rittenhouse Laboratory, Departments of Biochemistry and Biophysics and Department of Radiology, University of Pennsylvania, Philadelphia, Pennsylvania 19104-6396

M. Miwa
Hamamatsu Photonics, Sunamaya-cho, Hamamatsu, Japan

M. Ishii
Graduate Group in Bioengineering, University of Pennsylvania, Philadelphia, Pennsylvania 19104-6021

J. Schotland
Department of Radiology, University of Pennsylvania, Philadelphia, Pennsylvania 19104-6021

B. Chance
Department of Biochemistry and Biophysics, University of Pennsylvania, Philadelphia, Pennsylvania 19104-6021

J. S. Leigh
Department of Radiology, University of Pennsylvania, Philadelphia, Pennsylvania 19104-6021
(Received 21 December 1992)

Light propagation is measured through a multiple-scattering medium, and the scattering mean-free path is measured for different densities of scatterers. We analyze the effect of detector orientation relative to the light source, an effect of the anisotropy of the photon current. We compare light propagation in an infinite geometry to reflectance in a backscattering experiment. We compare to models for the boundary conditions applicable at the interface between the scattering medium and the adjacent free medium. These consist of linear combinations of absorbing and reflecting boundary conditions.

PACS number(s): 42.25.Fx, 42.68.Ay

I. INTRODUCTION

Light propagation through high-scattering media is a topic of recent interest [1]. Measurements of multiple-scattering light are used as tools to probe the structure of many different kinds of systems. The intensity of scattered light has been used to infer the density of dissolved polymers in shearing experiments [2]. The dynamics of scattered light have been of particular interest, as the observation of temporal fluctuations in transmitted light can be used to probe the motions of scattering centers within a sample [3]. These fluctuations of transmitted or backscattered light have given insight into the structure of heterogeneous particle mixtures, and may yield data on phenomena such as phase separation [4].

In biology, the transmission of light at different wavelengths has long been used to characterize the oxygen content of blood or tissue, making use of differences in optical absorption. Recent work has permitted measurements of O_2 content in systems that are strong scatterers of light [5]. However, such systems may have optical constants (scattering and absorption) that are not spatially uniform. This introduces a considerable degree of complexity in the interpretation of scattered-light measurements. A theory to interpret such data [6, 7] would also permit the physical mapping of absorption and/or scattering constants. Current experiments, however, have not generally provided consistent measurements of the effective mean-free path l^*, even in a homogeneous medium. In this work we determine l^* for suspensions of different concentrations of scatterers.

Important considerations for all light-scattering experiments include the geometry of the object, and the locations of the source and detector. Each of these affects the distribution of photon path lengths $P(s)$. In a dynamic correlation experiment, the Laplace transform of $P(s)$ is observed; in a pulse transmission or backscattering experiment, the observed pulse $u(t) = P(ct) = P(s)$ is equivalent to the distribution of path lengths. Thus an adequate understanding of $P(s)$ is necessary to interpret the data.

We demonstrate an effect due to the orientation of the detector relative to the source that affects $P(s)$ in many types of experiments. We compare data obtained in two different geometries, and in different orientations of detectors relative to sources in order to improve our understanding of these effects.

Related to the question of geometry is the question of the appropriate boundary condition to use at an interface between a scattering medium, and a medium in which

light propagates freely. One approach is to assume that such an interface is completely absorbing; an alternative approach is to consider that the boundary is described by a combination of absorbing and reflecting components. The ratios of these components may affect $P(s)$.

One appealing feature is that by modifying the ratio of absorbing to reflecting components, the presence of a mismatch in refractive index between the two optical media may be taken into account. It has been pointed out that possible internal reflections at the interface between two media affect $P(s)$ [8, 9]. However, the two published calculations for the magnitude of this effect disagree.

To address these questions, we study the propagation of backscattered light. By comparing our data to model functions, we determine the boundary conditions at the surface directly. The result is applicable to experiments other than our own (e.g., time-resolved transmission, time correlation experiments, and angular correlation of backscattered light).

II. EXPERIMENT AND DATA ANALYSIS

The experiment is illustrated schematically in Fig. 1 (inset). Laser pulses repeated at 5 MHz are injected via an optical fiber into a chamber containing a scattering suspension. Scattered light is collected from different positions in the medium by a second fiber (the detector fiber) and detected by a microchannel-plate detector (Hamamatsu R1712U- 11). Signals above set thresholds trigger a time-to-amplitude converter. The arrival time of each photon is measured with a resolution of 150 ps. A typical light pulse is shown in Fig. 1.

A commercial product, intralipid (IL), is the scattering agent. It is a white liquid consisting in large part of soybean oil (20%) suspended in water (80%). A small amount of egg yolk phospholipids stabilize the suspension.

The data contain pulses with source-detector separations between 3 and 6 cm. The fibers are centered in a $30 \times 30 \times 60$-cm^3 chamber. The separation between the source and detector is always less than the distance from either source or detector to the boundaries. Because we discount data collected at times greater than one-half the diffusion time from either the source or detector to the closest boundary, effects due to the finite volume of the aquarium are negligible.

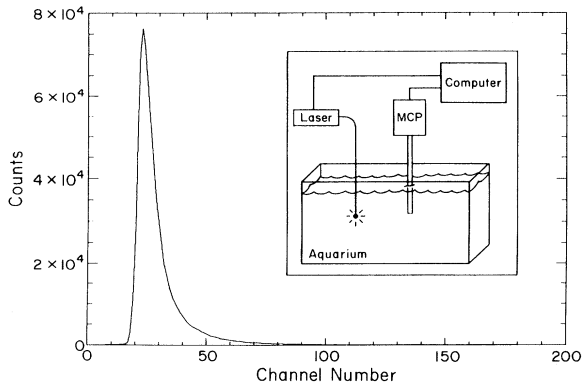

FIG. 1. Typical pulse is propagated through a high-scattering medium and observed as a function of time after the trigger. Inset: a schematic diagram of the apparatus.

We model the data using solutions of the diffusion equation to obtain the light-absorption coefficient μ_a and the scattering mean-free path l^*. The solutions for the diffusion equation give the hypothetical response for a point source and pointlike time resolution. However, the data are affected by the finite detector aperture (3.5 mm) and the actual detector response function. To match the models to the data we convolve the fitting function with a weighting function to account for the different aperture areas at different positions. We further convolve the fitting function with the measured instrumental response (the response of the detector to the laser in the absence of intervening scatterers).

In addition to l^* and μ_a, each pulse is characterized by two additional parameters: the absolute time offset t_0, and the throughput, both of which are unknown. Unfortunately, the efficiency of the microchannel plate changes in an unpredictable way with variations in the average incident flux. Thus the throughput must be determined for each separate source-detector separation.

The pulses are relatively featureless functions—lacking in nodes or other structure. Thus the space of fitting parameters describes a χ^2 surface with a shallow minimum at the best-fit solution, and parameters fit to a single source-detector position do not converge to a single limit. To overcome this problem we analyze data using multiple source-detector positions simultaneously. For a given concentration of scatterers, l^* and μ_a are unique, and must fit all data, regardless of the throughputs for each source-detector position. With this additional set of constraints, we derive consistent and reproducible scattering coefficients. We use typically four or five curves together to determine a single set of scattering and absorption parameters.

III. DISCUSSION

A. Effect of detector orientation

The photon density within a multiple-scattering medium is described by the diffusion equation:

$$\frac{\partial u}{\partial t} = D\nabla^2 u - \mu_a c u, \tag{1}$$

where u is the density of photons, μ_a is the absorption coefficient, and $D = cl^*/3$ is the photon diffusion constant. Because the filling fraction of the scatterer is small (0.1–0.5%) we neglect differences between photon phase velocity and energy transport velocity [10]. We use $c = 2.2587 \times 10^{10}$ cm s^{-1} for the speed of light in water. Note that the effective photon-scattering mean-free path l^* is related to the mean-free path l by the relation $l^* = l/(1 - \overline{\mu})$, where $\overline{\mu}$ is the average cosine of the single-particle scattering angle [11]. The effective mean-free path l^* describes the length scale over which scattering is isotropic.

For the homogeneous infinite medium the two-point Green's function is

$$u(r,t) = \frac{u_0}{(4\pi Dt)^{3/2}} \exp(-r^2/4Dt - \mu_a ct), \quad (2)$$

where u_0 is a constant, and r is the separation between source and detector. A central point of this article is that the observed light is *not* the photon density, it is the directional photon current $J_{\hat{r}}$ into the detector aperture. The current given by Fick's law, $J = -D\nabla u = J_{+\hat{r}} - J_{-\hat{r}}$ represents the *net* current only, not the directional current. The directional current represents the inward flow component perpendicular to the plane of a detector aperture. It may be obtained using transport theory [12] with the result

$$J_{\hat{r}} = \frac{c}{4}(u - \nabla_{\hat{r}} u/h), \quad (3)$$

defining the constant $h \equiv 3/(2l^*)$.

The physical interpretation is that the distribution of photons in the diffusion regime is somewhat anisotropic. The u component is the isotropic part of the photon flux, and the gradient term is the directional component. If there were no directional component, the photon distribution would be isotropic at every position, in which case there would be no tendency for photons to migrate outward from the source.

For the homogeneous and infinite medium, the application of (3) is particularly simple: we obtain

$$J = \frac{u_0 c}{4(4\pi Dt)^{3/2}} \exp(-r^2/4Dt - \mu_a ct)\left(1 + \frac{r\cos\theta}{ct}\right), \quad (4)$$

where θ describes the inclination of the detector (normal vector of the detector surface) towards the source-detector axis. In Fig. 2 we show two pulses observed with the same source-detector separation, but with detector orientations corresponding to $\theta = 0$ and $\theta = \pi/2$. In Fig. 3 we show the scattering mean-free path l^* determined separately for the detector in the $\theta = 0$ and $\theta = \pi/2$ orientations. The squares represent l^* determined by the experiment in which $\theta = \pi/2$. The triangles represent

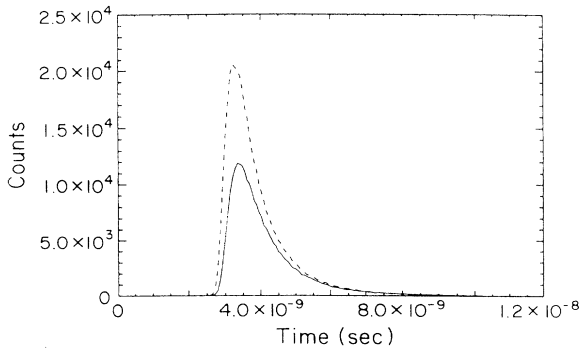

FIG. 2. Pulses propagated through 0.2% interlipid. The solid line indicates data taken such that the normal vector to the detector aperture is perpendicular to the source-detector axis ($\theta = \pi/2$). The dashed line indicates data taken with the detector facing the source ($\theta = 0$). Source-detector separation = 3 cm.

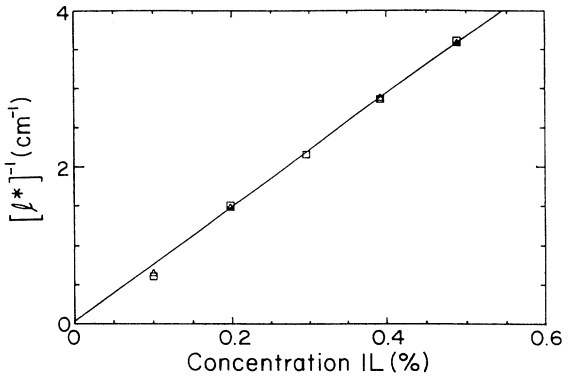

FIG. 3. $1/l^*$ for different concentrations of scatterers in the infinite-volume case. Squares represent data taken with the detector perpendicular to source; triangles represent data taken with the detector facing source.

l^* determined by an experiment in which $\theta = 0$. The only significant deviation from a straight-line fit is for the lowest dilution; in this case the minimum ratio of source-detector distance to mean-free path $L/l^* \approx 2.5$, where the diffusion equation is no longer applicable. In the next highest concentration, the minimum $L/l^* = 6$. Finally, we obtain $\mu_a = 0.025 \pm 0.002$ cm^{-1} for all concentrations of scatterers. This suggests that the scatterers are absorptionless, and the entire absorption is due to the water in which the scatterers are suspended. This is consistent with the tabulated absorption coefficient of water [13] at 775 nm, $\mu_a = 0.024$ cm^{-1}.

B. Boundary conditions at an interface with a free medium

Pulse propagation near the surface of a semi-infinite volume is discussed by several authors [8, 9, 3, 14]. Assume a surface at $z = 0$ divides a scattering medium ($z < 0$) from a medium in which light travels unhindered. In one approach [12] completely absorbing boundary conditions are assumed, $u|_{z=0} = 0$. The premise of this statement is the observation that the pulse shape even for light propagating near the surface of the semi-infinite volume appears only weakly dependent on the surface boundary conditions. In Fig. 4 we compare backscattering data for light that is free to radiate from the surface, to light that is absorbed everywhere except at the detector position. The absorbing condition is treated analytically by an image source with negative intensity at $z = -l^*$ together with the source at $z = +l^*$. The measured current at the surface is then [14]

$$J = \frac{u_0 l^*}{(4\pi D)^{3/2} t^{5/2}} \exp[-(r^2 + l^{*2})/4Dt - \mu_a^* ct]. \quad (5)$$

In Fig. 5 we compare free space transmission data (squares) to surface backscattering data (asterisks) as modeled by (5). The backscattering data show a consistent increase in $[l^*]^{-1}$ with higher concentrations of scatterers, but do not agree well with the bulk transmission data.

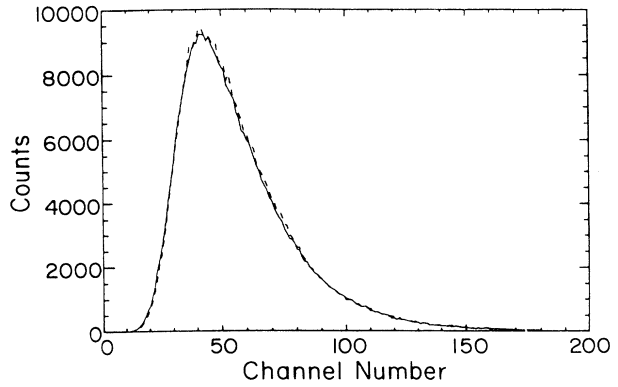

FIG. 4. Surface transmission data for light with radiation conditions (solid line) and absorbing boundary condition (dashed line).

A second approach to photon diffusion across a plane surface is to adopt the boundary condition inferred from transport theory, previously used to interpret directional currents. For the semi-infinite volume containing scatterers for all $z < 0$, the directional current at the surface is $J_{-z} = 0$. That is, no light that leaves the scattering medium returns. However, a finite density of photons is permitted at the $z = 0$ surface, and the boundary condition is

$$uh + \frac{\partial u}{\partial z} = 0. \tag{6}$$

There is a subtle distinction between this case and the absorbing condition $u|_{z=0} = 0$. The first statement is about photon *flux*; the second statement is about photon *number density*. The second statement is an approximation that describes the photon density at positions sufficiently far from the surface. It is mathematically simpler. The first statement, however, is more readily

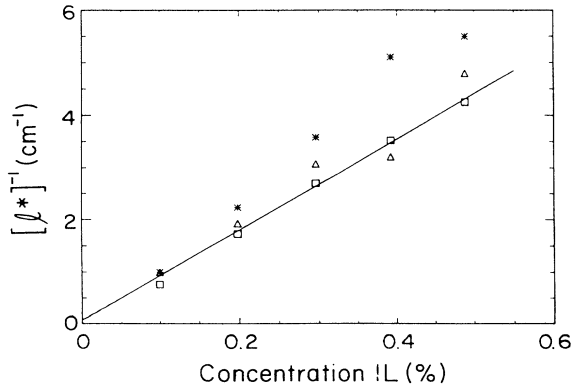

FIG. 5. $1/l^*$ for bulk transmission (squares) compared to surface backscattering data fit assuming pure absorbing boundary conditions at surface (asterisks); surface backscattering data fit assuming mixed boundary conditions (triangles). The solid line represents the best fit to l^* determined in bulk transmission only (squares).

adapted to the case where there is a mismatch in the index of refraction between the scattering medium and the free medium. Others have suggested [8, 9] that such a mismatch changes the boundary condition, which may in turn modify the distribution of photon path lengths.

If there are internal reflections at the interface, they may be described as an incoming current J_-, related to the outgoing current J_+ by $J_- = RJ_+$, where R is an effective reflection coefficient. This is in turn related [9] to the boundary-value coefficient h by

$$h = \frac{3}{2l^*}\frac{R-1}{R+1}, \tag{7}$$

where

$$h = \frac{1}{l^*}\frac{1/2 - C_1}{1/3 + C_2}; \tag{8}$$

$$C_1 \equiv \int_0^{\pi/2} d\theta\, R(\theta) \sin\theta \cos\theta, \tag{9}$$

$$C_2 \equiv -\int_0^{\pi/2} d\theta\, R(\theta) \sin\theta \cos^2\theta. \tag{10}$$

The coefficient $R(\theta)$ is the surface reflectivity averaged over the two polarization components. Thus, h depends on the relative mismatch of refractive index.

For water ($n = 1.33$ for incident light $\lambda = 780$ nm) we calculate $h = 0.6/l^*$, consistent with the values tabulated in Zhu, Pine, and Weitz [9]. We introduce $\Delta \equiv (hl^*)^{-1}$ to eliminate explicit dependence on l^*. We calculate $\Delta = 1.68$ from the above equations.

Given the boundary condition (6) for the semi-infinite volume, the two-point Green's function is [15]

$$u(r,t) = \frac{u_0 \exp(-r^2/4Dt - \mu_a ct)}{(4\pi Dt)^{3/2}} \times[1 - h\sqrt{\pi Dt}\,\mathrm{erfc}(h\sqrt{Dt})\exp(h^2 Dt)]. \tag{11}$$

For simplicity both source and detector are located at the surface, separated by distance r (analysis showed that when the initial scattering event took place within an exponential distribution of mean depth $z = l^*$ of the surface, the change to the best fit parameters was less than one part in 10^3). A further simplification arises because at the surface the photon current and density differ only by a fixed constant. Thus we fit (11) to the data directly.

In Fig. 5 we compare the mean-free path obtained from surface backscattering data fit by (11) (triangles) to those values obtained in the infinite-volume case (squares). The agreement between the two data sets is significantly better than that afforded by the assumption of pure absorption boundary conditions. The absorption constant $\mu_a = 0.026 \pm 0.003$ cm^{-1}, consistent with measurement in the bulk case, as well as μ_a determined by fits using the model of Eq. 5.

A third approach to the boundary condition is outlined by Freund [8] using Milne theory. He obtains mixed boundary conditions, but with the parameter $\Delta = 1/hl^*$

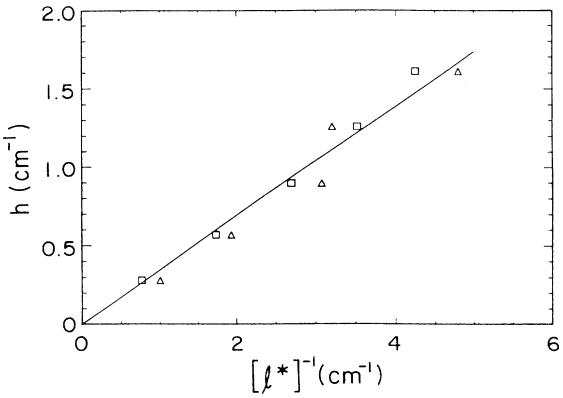

FIG. 6. Boundary-value parameter $h = 1/\Delta l^*$ for different concentrations of scatterers. Squares represent the assumption that l^* determined in bulk is the correct value; triangles represent the assumption that l^* determined in surface backscattering is the correct value.

given by

$$\Delta = \frac{2(1+R)}{3(1-R)}\phi(R), \qquad (12)$$

$$\phi(R) = \frac{1-\frac{3}{16}(1-R)}{1-\frac{2}{3}(1-\ln 2)(1-R)},$$

where $R = 0.488$ is the average reflectivity in the present case (water-air interface). From (12) we calculate $\Delta = 1.94$. This theory is distinguishable from transport theory only by the value of h that is fit to the data.

Because we obtain values for h from the data we are able to test the above theories quantitatively. In Fig. 6 we plot values of h measured for the different concentrations of scatterers. The parameter h scales with $1/l^*$, as predicted by both models. We obtain $\Delta = 2.9 \pm 0.2$ experimentally. This is not in agreement with either model.

Freund argues that $h = (\Delta l)^{-1} \neq (\Delta l^*)^{-1}$. That the ratio l^*/l depends only on the size and dielectric constant of the particles, an experiment using spheres of a known radius could be informative. Using a phase contrast microscope, we could observe rapidly moving particles of different sizes. That the particles can be seen at all implies that they are at least as big as the wavelength of light, which in turn implies that the single-particle scattering is anisotropic. Thus, it is likely that $l^* \gg l$. If this argument is correct, the data would be in even worse agreement with the two calculations for Δ.

IV. CONCLUSIONS

We obtain measurements of l^* from optical pulse propagation in scattering media in both transmission and backscattering geometries. By changing the orientation of the detector relative to the source in the transmission geometry, we measure *different* pulse shapes, consistent with transport theory, from which we obtain identical values of l^*. This suggests that the transport theory gives an adequate explanation of photon transport, at least far from an interface.

The backscattering data provide measurements of l^* consistent with the transmission measurements. This suggests that mixed boundary conditions are present at the surface. The ratios of the components (reflecting to absorbing) scale as expected with increasing scatterer density; however, there is a significant discrepancy between the ratios of the measured components with respect to transport and Milne theories. This suggests that phenomenological approaches, such as Milne and transport theories, give a qualitative description but miss some of the physics present at the interface between a multiple scattering medium and a free medium.

ACKNOWLEDGMENTS

We are grateful to Peter Kaplan and David Pine for helpful discussions. This work was supported by NIH Grant Nos. HL44125 and HL07614.

[1] *Scattering and Localization of Classical Waves in Random Media*, edited by P. Sheng (World Scientific, Singapore, 1990).
[2] P. K. Dixon, D. J. Pine, and X. Wu, Phys. Rev. Lett. **68**, 2239 (1992).
[3] D. Pine, D. Weitz, J. Zhu, and E. Herbolzheimer, J. Phys (Paris) **51**, 2101 (1990).
[4] P. D. Kaplan, A. G. Yodh, and D. J. Pine, Phys. Rev. Lett. **68**, 393 (1992).
[5] E. Sevick, B. Chance, J. Leigh, S. Nioka, and M. Maris, Anal. Biochem. **195**, 330 (1991).
[6] J. Schotland, C. Gonatas, and J. Leigh (unpublished).
[7] J. Schotland, J. Haselgrove, and J. Leigh, Appl. Opt. **32**, 448 (1993).
[8] I. Freund, Phys. Rev. A **45**, 8854 (1992).
[9] J. Zhu, D. Pine, and D. Weitz, Phys. Rev. A **44**, 3948 (1991).
[10] M. van Albada, B. van Tiggelen, A. Lagendijk, and A. Tip, Phys. Rev. Lett. **66**, 3133 (1991).
[11] A. Ishimaru, *Wave Propagation and Scattering in Random Media* (Academic, San Diego, 1978), Vol. 1.
[12] S. Glasstone and M. Edlund, *Elements of Nuclear Reactor Theory* (Van Nostrand, New York, 1952).
[13] G. Hale and M. Querry, Appl. Opt. **12**, 555 (1973).
[14] M. Patterson, B. Chance, and B. Wilson, Appl. Opt. **28**, 2331 (1989).
[15] H. S. Carslaw and J. C. Jaeger, *Conduction of Heat in Solids* (Oxford University Press, Oxford, 1959).